CONCRETE RESEARCH LETTERS

www.crl.issres.net Vol. 3 (3) Sept. 2012

Pre- and Post-Fire Strength Assessment of Ferrocement beams

Yousry B. I. Shaheen, Zeinab A. Etman[C] and Ahmed G. Ramadan
Department of Civil Engineering, Faculty of Engineering,
Mnoufiya University, EGYPT.

Abstract

The results of an experimental investigation on the behavior of ferrocement beams after exposed to fire are presented in this paper. Different types of steel meshes are used compared with conventional reinforcement. The experimental program comprised casting and testing of eighteen beams having the dimensions of 100mm×100mm×1000mm. Three beams were reinforced as a conventional reinforcement. Each control beam was reinforced with two steel bars of diameter 8 mm in tension, two steel bar of diameter 6mm in compression and stirrups of 6 mm diameter placed at 200 mm intervals. The ferrocement beams were reinforced with steel meshes without any stirrups. Two types of steel meshes were used to reinforce the ferrocement laminate. These types are: square welded wire fabric, and expanded wire mesh. Single layer, double layers and three layers of square welded wire mesh were employed. Single layer and double layers of expanded wire mesh were employed. The experimental program was classified into three groups. First group was tested without exposure to fire, the second group was tested after exposure to fire for six hours and the last group was tested after exposure to fire under loading. All specimens were tested under 4-points flexural loadings. The performance of the test beams in terms of strength, stiffness, cracking behavior and energy absorption was investigated. The results showed that high serviceability and ultimate loads, crack resistance control, and better deformation characteristics could be achieved by using the proposed ferrocement forms.

Keywords: Ferrocement beams; RC beams; Steel mesh; Polypropylene fibers; Ultimate load; Cracking; Serviceability load; Ductility ratio; Energy absorption; Fire.

1. Introduction

Ferrocement is a form of reinforced concrete that differs from conventional reinforced or prestressed concrete primarily by the manner in which the reinforcing elements are dispersed and arranged. It consists of closely spaced, multiple layers of mesh or fine rods completely embedded in cement mortar. The Ferrocement is a building material with evident advantages for thin-walled members and spatial structures for this type of material. For their properties, the ferrocement is recommended to be used for curves and folded thin elements with a rigidity due to the form and not to the quantity of the material. The use of ferrocement is a promising technology for

[C] corresponding Author: Zeinab A. Etman, Lecturer in civil engineering
E-mail:dr_zeinab_2006@yahoo.com Telephone: +201009727355 Fax: +20482238232

increasing the flexural strength of deficient reinforced concrete members. A large number of civil infrastructures around the world are in a state of serious deterioration today due to carbonation, chloride attack, etc. Moreover many civil structures are no longer considered safe due to increase load specifications in the design codes or due to overloading or due to under design of existing structures or due to lack of quality control. While most ferrocement housing applications have been directed toward low-cost housing solutions; excellent quality, durable, well finished, and serviceable housing products can be readily produced with ferrocement. These products encompass various structural elements such as walls, beams, slabs and roofing systems. Moreover, ferrocement has also been used as a repair material for concrete elements. Many investigators have reported the physical and mechanical properties of this material and numerous test data are available to define its performance criteria for construction and repair of structural elements. Rajkumar D. and Vidivelli B. [1] studied the mechanical properties of mortar through difference in polymer content and also by ferrocement with three different volume fractions of mesh reinforcement incorporated by Styrene Butadiene Rubber Latex. Consequently in order to exercise proper quality control from materials point of view, the ferrocement specimens being intended from Ferrocement Model Code and in addition to that the results were checked through the limitations of relevant code. Al-Rifaie et al. [2] presented the results of an experimental and theoretical study of the behavior of cannel shaped ferrocement one-way bending elements. The results showed that this type of elements can undergo large deflections before failure and is suitable for construction of horizontally spanning unit for one-way bending. Presented the use of the ferrocement technology in developing ferrocement sandwich and cored panels for floor and wall construction [3-6]. Retrofitting using Ferrocement is gaining popularity in India and other developing nations due to its high strength to weight ratio and ease of construction [7]. A number of studies have been conducted worldwide by research scholars, engineers, concrete technologists, etc. to evaluate the performance of beams retrofitted using various materials. Fire remains one of the most serious potential risks to most buildings and structures. Most structural materials which are weakened when exposed to high temperatures cause buildings to collapse. Therefore, the use of fire protection materials to reduce thermal damage of structural members is important and necessary. Ferrocement is one of the cementitious composite materials, which is constructed of cement mortar reinforced with close spaced layers of continuous and relatively small sized wire mesh [8-9]. Since mortar is a good insulator and the reinforcing wire mesh could reduce surface spalling, consequently using ferrocement jacketing for strengthening of structural components like reinforced concrete, prestressed concrete, or steel could enhance the fire resistance of the composite elements. Djaknoun S., et al. [10] presented high strength concrete mortars with very fine sand exhibits a typical quasi-brittle behavior. Fracture mechanics approach is useful engineering tool for analysis of specific structural members where cracking is a governing design criteria. Greepala V. et al. [11] analyzed the specific heat capacity of ferrocement at elevated temperatures of up to 800°C based on time-varying surface temperature during fire exposure and its temperature-dependent thermal conductivity using inverse thermal analysis approach. The specific heat capacity of ferrocement was slightly higher than those of concrete cover given by Euro Code (ACI Committee 549.2R) [12-13], hence ferrocement can be used as fire protection material because it can absorb more heat than concrete cover. An increase in wire mesh content cause slightly decrease in specific heat capacity of ferrocement at low temperature, however at the first Peak the specimen which has volume fraction of 1.63% show the highest specific heat. Greepala V. and Nimityongskul P. [14] presented study on sandwich-sample to simulate the actual conditions of exposure to fire. The results showed that, using

ferrocement jacket was a satisfactory solution for fire protection due to its post-fire strengths as compared with those of plain mortar. An increase in wire mesh content significantly improved the mechanical properties of ferrocement under normal condition; however after fire exposure the content of wire mesh was no longer significant regardless of heating duration. Greepala V. and Nimityongskul P. [15] presented an integrity and insulation performance of ferrocement exposed to fire for 3 hours in accordance with ASTM E-119 standards [16]. The results showed that; the maximum crack width of ferrocement specimen decreased as a thickness of ferrocement increased. Moreover, the increase in mortar covering led to an increase in maximum crack width. The increase in thickness had less influence on the insulation performance of ferrocement. So ferrocement specimens met the structural integrity criterion in accordance with ASTM standard. This paper presents the results of experimental investigation to on the assessment of ferrocement beams pre and post fire

2. Fire resistance

The ability of a structural element to resist a fire defines as a fire resistance. There are many factors depend on the resistance of concrete elements such as; the fire severity, geometry, support condition and the material of the element. Some standards that are commonly used for fire resistance tests such as ISO TR 834-3:2012, ASTM E119-12 and BS 476-10:, 2009 [16-18]. ISO TR 834-3:2012 [17] is used by many countries and some national standards are based on this. Similar standards are used by most European countries, while the British use the BS 476-10, 2009 standard [18]. The United States use ASTM E119-12 [16].

3. Test Furnace

Furnace was especially constructed for the experimental work. The 1500 x 750 x 200 cm thick wall. The walls are detached bricks as two layers with an isolated material between the two layers. Ceramic fiber blanket was used to control the heat flow through ferrocement specimen. The temperature on the unexposed side of the sample was monitored by eight thermocouples. The thermocouples used were type K which can be used for temperature rang 0 to 900°C. The accuracy of thermocouples has been found ±0.1°C. The temperature of the furnace reached up to 943.33 ºC within a time 3 hours. Figure (1) shows the interior temperature inside the furnace according to ASTM E119-12 [12]. Three burners at the exposed surface specimens were used. Thermocouples types T were used to control the temperature in accordance with ASTM E119-12 [12]. Proportional integral differential (PID) (Temperature controller) was used for determining the measurable temperature. The furnace was being kept at constant temperature during the beams exposed to fire. Figure 2 shows the ferrocement specimens inside the furnace.

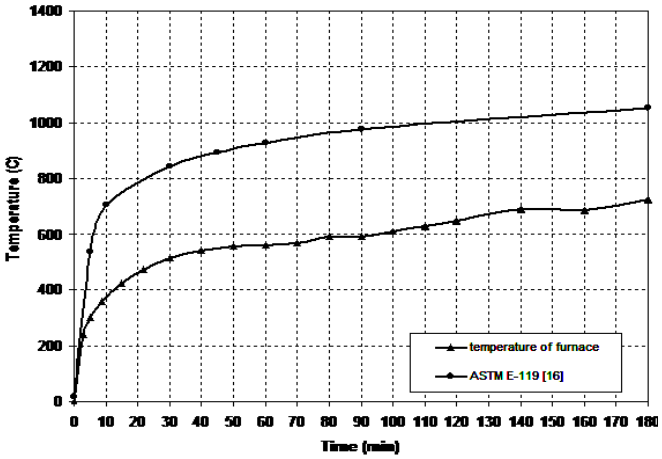

Figure 1. Heating Curve of Testing Furnace

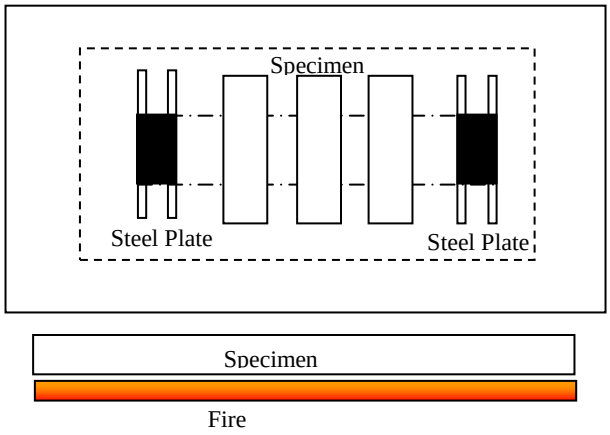

Figure 2. Ferrocement Specimens inside furnace

4. Experimental program

The experimental program was designed to investigate the behavior and strength of ferrocement beams when exposed to fire. To achieve this aim, the experimental program comprised casting and testing of eighteen beams of dimensions 100 mm×100 mm×1000 mm. three beams were reinforced as a conventional reinforcement. Each control beam was reinforced with two steel bars of diameter 8mm in tension, two steel bar of diameter 6mm in compression and stirrups of 6 mm diameter placed at 200 mm intervals. The ferrocement beams were reinforced with steel mesh without any stirrups. Two types of steel meshes were used to reinforce the ferrocement laminate. These types are: square welded wire mesh, and expanded wire mesh. Single layer, double layers and three layers of square welded wire mesh were used. Single layer and double layers of expanded wire mesh were used. Generally all the meshes are used galvanized. The details of the test specimens are given in Table 1, while the cross sections of the different designations are shown in Figure 3. Figure 3 depicts the typical steel wire meshes used in ferrocement applications

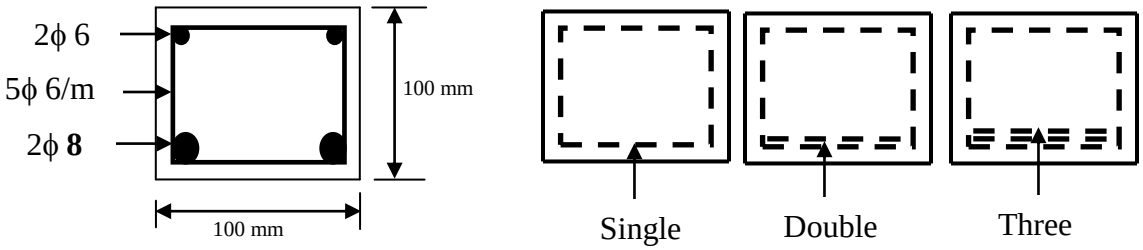

a) Control beams

b) Beams with ferrocement form reinforced with single or double layers or three of steel mesh

Figure 3. Cross Section of the Test Beams

TABLE 1: DETAILS OF THE TEST SPECIMENS

Group Number	Designation of Beam Samples	Reinforcing Steel Mesh In the Ferrocement				Steel Reinforcement			Total Weight of Steel (kg)
		Type	No. of Layers	Thickness (mm)	Volume Fraction (%)	Tens	Comp	Stirrups	
A (Unheated)	CON. A	--	--	25	--	2ϕ8	2ϕ6	5ϕ6/m	2.050
	1 EX. A	Expanded mesh	1	20	1.73	--	--	--	0.550
	2 EX. A	Expanded mesh	2	25	2.76	--	--	--	0.950
	1 WE. A	Square welded mesh	1	20	1.64	--	--	--	0.800
	2 WE. A	Square welded mesh	2 (tens.)	25	2.63	--	--	--	0.950
	3 WE. A	Square welded mesh	3 (tens.)	30	3.29	--	--	--	1.200
B (Exposed to fire for 6 hours under loading)	CON. B	--	--	25	--	2ϕ8	2ϕ6	5ϕ6/m	2.050
	1 EX. B	Expanded mesh	1	20	1.73	--	--	--	0.550
	2 EX. B	Expanded mesh	2	25	2.76	--	--	--	0.950
	1 WE. B	Square welded mesh	1	20	1.64	--	--	--	0.8oo
	2 WE. B	Square welded mesh	2 (tens.)	25	2.63	--	--	--	0.950
	3 WE. B	Square welded mesh	3 (tens.)	30	3.29	--	--	--	1.200
C (Exposed to fire for 6 hours)	CON. C	--	--	25	--	2ϕ8	2ϕ6	5ϕ6/m	2.050
	1EX. C	Expanded mesh	1	20	1.73	--	--	--	0.550
	2EX. C	Expanded mesh	2	25	2.76	--	--	--	0.950
	1WE. C	Square welded mesh	1	20	1.64	--	--	--	0.800
	2WE. C	Square welded mesh	2 (tens.)	25	2.63	--	--	--	0.950
	3WE. C	Square welded mesh	3 (tens.)	30	3.29	--	--	--	1.200

The beams were divided into three groups according to fire. First group (A) was tested without exposure to fire. In this group, one beam was cast with ordinary formwork. This beam was reinforced with two steel bar of 8 mm diameter at the tension side and two steel bars of 6 mm at the compression side as well as shear reinforcement (Stirrups) of 5ϕ 6/m. The other beams in the group were reinforced with steel meshes. No reinforcing bars at the compression or tension side or stirrups were used in these beams. The second Group (B) was tested after exposure to constant value 400 °C for six hours. The last group was tested after exposure to fire under loading. A uniform load is applied on the beams (group C) during the beams exposed to fire at 400°C. About 30 % of ultimate load was used as uniform load during fire. All specimens were tested under 4-points flexural loadings.

5. Design equations for reinforced concrete specimens:

Current design codes adopted different equations for reinforced concrete beams subjected to bending, based on beam moments. The ACI 318-2011 [19] code presented detailed equations for calculating the factored moments, and flexural reinforcement, the required compression reinforcement is given by:

The nominal moment strength of:

$$M_n = (\rho - \rho^-) f_y \left(1 - 0.59 \frac{\rho f_y}{f_{cy}}\right) bd^2 + \rho^- bd f_y \left(d - d^-\right) \quad (1)$$

in which M_n is the nominal moment ($M_n = P_n L/6$, L is the clear span= 900 mm), ρ, ρ^- is the reinforcement ratio (ρ = 0.0126 and ρ^- = 0.007), f_y is the yield strength of the tension and compressive reinforcement respectively (f_y = 307.7 and 332.3 MPa,), f_{cy} is the 28-day cylinder compressive strength, b is the width of the beam cross section (b = 100 mm) and d is the effective depth (d = 80 mm).

6. Design equations for ferrocement specimens:

Current design codes adopted different equations for reinforced concrete beams subjected to bending, based on strength or working stresses. This analysis is similar to the analysis of reinforced concrete Beam. The ACI 549.1R-99 [12] code presented detailed equations for calculating the volume fractions, nominal moment capacity for ferrocement specimens.

The volume fraction represented by (N) layers of expanded metal mesh and welded wire mesh according to ACI 549.1R-99.

$$V_f = \frac{N \pi d_b^2}{4h} \left(\frac{1}{D_l} + \frac{1}{D_t}\right) \quad (2)$$

Where:

N is the number of layers of mesh reinforcement, d_b is the diameter of mesh wire, h is the thickness of ferrocement, D_l is the center-to-center spacing of wires aligned longitudinally in reinforcing mesh, D_t is the center-to-center spacing of wires aligned transversely in reinforcing mesh; as illustrated in table (1) and (2) .

The nominal moment capacity are factored the volume fraction and the moment capacity occurring simultaneously at the section considered. According to ACI 549.1R-99, the moment capacity can be calculated as follow:

$$M_n / (f_{cy} b h^2 \eta) = 0.005 + 0.422 V_f f_y / f_{cy} - 0.0772 (V_f f_y / f_{cy})^2 \quad (3)$$

in which M_n is the nominal moment ($M_n = P_n L/6$, L is the clear span= 900 mm), f_y is the yield strength of the expanded and welded wire mesh respectively (f_y = 315.5 and 453 MPa,), f_{cy} is the 28-day cylinder compressive strength, b is the width of the beam cross section (b = 100 mm) and d is the effective depth (d = 80 mm), η ia the global efficiency factor of reinforcement (η = *0.5*). For simplified solution; a graphical solution according to ACI 549.1R-99 [12] was used to calculate the nominal moment (M_n).

.

7. Mix design and material properties

Mortar was used for producing the ferrocement beams. The mortar consisted of sand and ordinary Portland cement with a sand-cement ratio of 2.0. To improve the properties of the mortar, 10% of the cement was replaced by silica fume. The used water-cement/silica fume ratio was 0.30 and superplasticizer with ratio of 2.0% by weight of (cement + silica fume) was used to improve workability. The polypropylene Fibers was used as improver to tensile strength, increaser to workability and provender to appear shrinkage crack as it is spread in all directions besides it is high chemical resistance. Table 2 shows the mix proportion of mortar used. For each mortar mix, three cubes of dimensions 100 x100 x 100 mm were cast and tested after 3, 7, 14 and 28 days to determine the mortar compressive strength. Table 3 shows the average mortar compressive strength for the trail mortar. Table 4 shows the average mechanical properties at 3, 7, 14, and 28 days for the used mix of mortar for the three groups. Mild steel wire mesh (Expanded and square wire mesh), Figure 4 was used in fabricating the ferrocement beams in the three groups. The geometric properties of these two types of steel mesh are given in Table 5. Mild steel was used for the reinforcing bars and the stirrups in the control beams. The nominal yield and tensile strength for this type of steel are 360MPa and 520MPa respectively.

TABLE 2: MIX PROPORTION OF MORTAR

cement : Sand	1:2
Sand	Passing through sieve with aperture 2mm
SF	10% of cement by weight
Polypropylene fiber	2500 g/m
Water-dry mix ratio	30%
Superplasticizer	2% of total binder by weight

TABLE 3: COMPRESSIVE STRENGTH OF THE TRAIL MORTAR

Code mix	3 days		7 days		14 day		28 day	
	P_{av} (kN)	F_{cu} (N/mm^2)	P_{av} (kN)	F_{cu} (N/mm^2)	P_{av} (kN)	F_{cu} (N/mm^2)	P_{av} (kN)	F_{cu} (N/mm^2)
A	30	3	245	24.5	265	26.5	280	28
B	200	20	248	24.8	280	28	350	35
C	200	20	300	30	350	35	410	41
D	190	19	295	29.5	330	33	370	37
E	80	8	275	27.5	290	29	320	32

TABLE 4: MECHANICAL PROPERTIES OF USED MORTAR

Mechanical properties	Nature of sample	3 days		7 days		14 days		28 days	
		P_{av} (kN)	Strength (MPa)	Pav (kN)	Strength (MPa)	P_{av} (kN)	Strength (MPa)	P_{av} (kN)	Strength (MPa)
Compressive strength (F_{cu})	cube (100x100x100mm)	212	21.2	300	30	3.2	35.2	415	41.5
Flexural Strength (F_f)	prism (500x100x100mm)	9.2	3.68	12.5	5	13.7	5.48	16	6.4
Splitting tensile strength (F_{sp})	cylinder (100x50mm)	25.5	.0814	33	.015	50	.159	52	.165

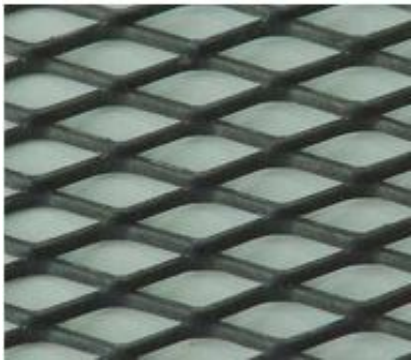

a) Expanded mesh

b) Square welded wire mesh

Figure 4. Types of Steel Mesh

TABLE 5: GEOMETRIC PROPERTIES OF THE STEEL MESHES

Mesh Type	Mesh Opening (mm)		Dimension of Strands (mm)		Diameter (mm)	Grid Size (mm)	Weight (kg/m^2)
	Long Way	Short Way	Width	Thickness			
square welded wire fabric	30	30	--	--	2.5	30x30	2
Expanded (metal) mesh	30	13	2.40	1.25	2	30x13	1.375

8. Preparation of test specimens

To cast ferrocement beams, a special wooden mold as shown in figure 5, was used. The mold was designed and manufactured to facilitate the assembling process at the time of casting the forms and to ease the disassembling after casting and hardening. All test specimens have the same dimensions. The overall height for all specimens equals 100 mm and the width is 100 mm, the overall length for all specimens equals 1000 mm, and the effective span is 900 mm. The

specimens have overhangs of 50 mm from each end. These overhangs were also required to accommodate the support assemblies. The ferrocement beams were prepared in the following sequence:

1. The wooden mold was assembled and the reinforcing steel mesh was formed and placed in each vent of the mold. The constituents of the mortar were mixed and cast in each vent to the required thickness as shown in Figure 5.
2. The ferrocement forms were left for 24 hours in the mold before disassembling the mold. At the end of this step, five ferrocement beams are produced.
3. The ferrocement forms were wet curing for 28 days. Visual inspection of the ferrocement beams showed that no cracks were developed during the curing period.

Figure 5. The Wooden Mold

9. Test Setup

After 28 days, the specimen was painted with white paint to facilitate the crack detection during testing process. Flexural testing machine of 100 kN capacities was used. The test was conducted under a four-points loading shown in Figure 6. The specimen was centered on the testing machine, where the span between the two supports was kept constant at 900 mm. A dial gauge with an accuracy of 0.01 mm was placed under the specimen at the center to measure the deflection versus load. Load was applied at 5 kN increments on the specimen. Concurrently, the beam deflection was determined by recording the dial gauge reading at each load increment. Cracks were traced throughout the sides of the specimen and then marked with black markers. The first crack-load of each specimen was recorded. The load was increased until complete failure of the specimen was reached.

10. Experimental results

The test results are listed in Table 6. The table shows the obtained experimental results for each specimen as well as the average ultimate failure load, the first crack load, service load, ductility ratio, and energy absorption properties for each group. Ductility ratio is defined here in this investigation as the ratio between the mid-span deflection at ultimate load to that at the first crack load (Δ_u/Δ_i), while the energy absorption is defined as the area under the load-deflection curve. Computer program (BASIC language) was used to calculate the area under curve by integrated the equation of the load-deflection curve for each beam specimens as follow:

$Energy\ absorbed = \int_0^{\Delta_u} L(\Delta) d\Delta$; Where L (Δ) is the equation of load-deflection curve, and Δ_u is the mid-span deflection at ultimate load

Service load, or flexural serviceability load, is defined as the load corresponding to a deflection equal to span/350.

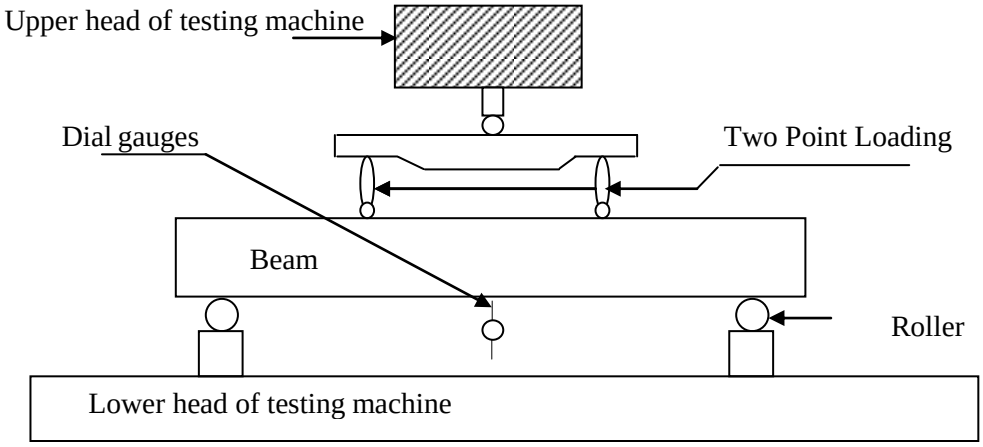

Figure 6. Testing Machine and Test Set-up

For all test specimens incorporating ferrocement forms, the total weight of the reinforcing with the steel meshes was less than that used for those of the control beams in the form of the top bars, bottom bars, and stirrups. The saving in the steel weight, relative to the control beams, ranged from 41.5 % to 73.2% depending on the type of the steel mesh and the number of steel mesh layers in the ferrocement forms.

The load-deflection curves of the test specimens are shown in Figures 7, through 9. The load-deflection relationship can be divided into three regions: a) linear relationship up to first cracking of concrete, b) transition region where the relation deviated from linearity due to continuous cracking of the beam, c) large plastic deformation due to yielding of the reinforcing steel bars and the steel mesh. The load at which the load-deflection relationship started to deviate from the linearity and the extent of the plastic deformation varied with the type of steel mesh in the ferrocement beams.

It can be seen from Figure 7 that the initial stiffness of the beams incorporating ferrocement forms reinforced with expanded steel mesh (1 EX) is equal to that of the control beams and higher than the beams reinforced with other types of steel mesh. In Figure 8, the initial stiffness of the beams incorporating ferrocement forms reinforced with expanded steel mesh (2 EX) is higher than that of the control beams and the beams reinforced with other types of steel mesh. In Figure 9 the initial stiffness of the control beams is higher than that of the beams reinforced with any type of steel mesh.

TABLE 6. TEST RESULTS OF TESTED BEAMS

	Designation	First Crack Load (kN)	Service Load (kN)	Ultimate Load (kN)	M_{exp} (kN.mm)	M_n* (kN.mm)	Deflection (mm)		Ductility Ratio (Δ_u/Δ_i)	Energy Absorption (kN.mm)
							Δ_i	Δ_u		
Group (A)	CON. A	4.3	6.42	10.8	1620	2064.4	2.28	29.81	13.07	269.8
	1 EX. A	1.08	1.58	2.71	406.5	412.84	1.47	12.61	8.58	27.0996
	2 EX. A	2.32	3.29	5.8	870	878.01	2.89	21.3	7.37	99.71
	1 WE. A	0.91	1.46	2.56	384.58	389.9	2.02	9.69	4.797	16.13
	2 WE. A	2.09	3.29	5.58	836.37	842.17	2.19	14.17	6.47	56.96
	3 WE. A	3.47	5.09	9.021	1353.2	1367.51	2.59	16.27	6.26	100.52
Group (B)	CON. B	3.31	4.96	8.8	1320	2015	1.7	19.56	11.51	140.793
	1 EX.B	0.89	1.37	2.54	381	373.15	1.28	9.57	7.48	18.393
	2 EX. B	1.9	2.82	4.92	738	725.56	1.73	11.42	6.6	42.596
	1 WE. B	0.84	1.28	2.28	341.6	356.56	1.35	9.88	7.32	17.694
	2 WE. B	1.73	2.79	4.68	702.0	712.6	1.69	10.91	6.45	36.32
	3 WE. B	2.55	4.23	7.0	1050	1082.13	1.98	10.75	5.42	48.918
Group (C)	CON. C	3.06	4.42	8.34	1251	2015	1.95	19.56	10.03	130.257
	1EX. C	0.88	1.37	2.33	349.6	373.15	1.7	8.84	5.17	14.4175
	2EX.C	1.83	2.74	4.76	713.94	725.56	1.78	10.42	5.85	35.868
	1WE. C	0.78	1.27	2.05	307.5	356.56	1.34	7.48	5.58	10.063
	2WE. C	1.77	2.77	4.66	698.76	712.6	1.93	8.25	4.27	24.957
	3WE. C	2.46	3.91	7.03	1054.61	1082.13	1.95	9.16	4.697	41.867

* M_n: nominal moment strength According to ACI [12,19]

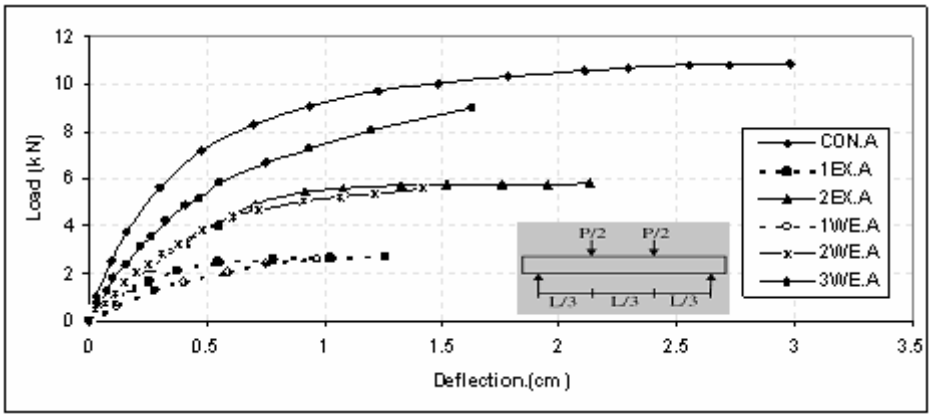

Figure 7.Load deflection curves for control beam and Ferrocement test specimens (Group A).

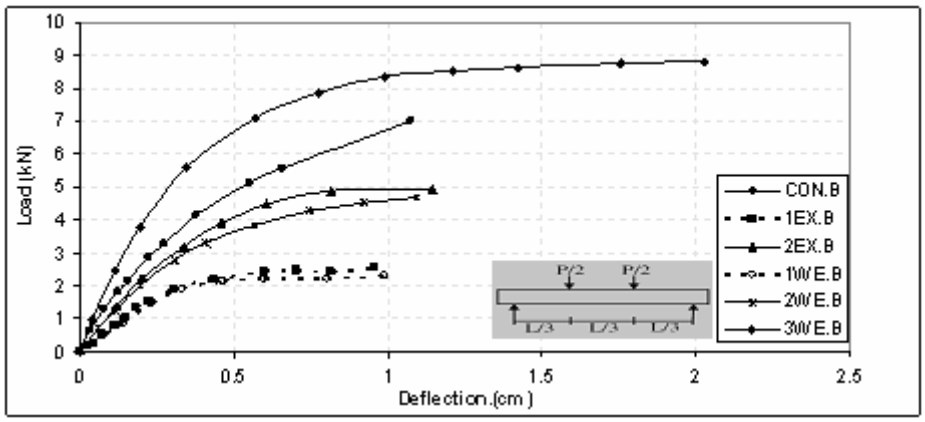

Figure 8. Load-deflection curves for control beam and Ferrocement test specimens (Group B).

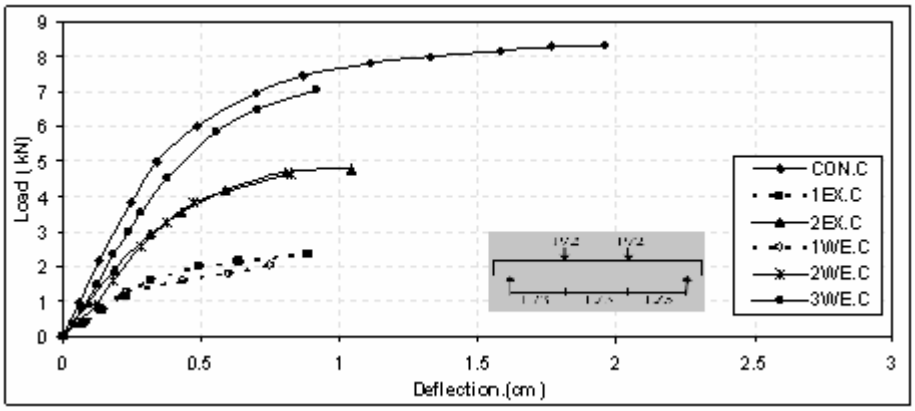

Figure 9: Load-deflection curves for control beam and Ferrocement test specimens (Group C).

10.1 First Crack Load and Serviceability Load

The first crack load was determined during the test, while the flexural serviceability load was determined for the test specimens from the load deflection curves shown in Figures 7, 8, and 9. The results given in Table 6 show that all beams incorporating permanent steel forms achieved lower first crack load and serviceability load than those of the control specimens. The beams reinforced with expanded (EX) steel mesh had the highest serviceability load followed by those reinforced with square meshes regardless of the number of steel layers. For the same type of steel mesh, beams with three layers of steel mesh layers achieved higher first crack load and serviceability load than those with double steel mesh layer and single steel mesh layer. Figures 9 and 10 show the first crack load and service load for all tested beams.

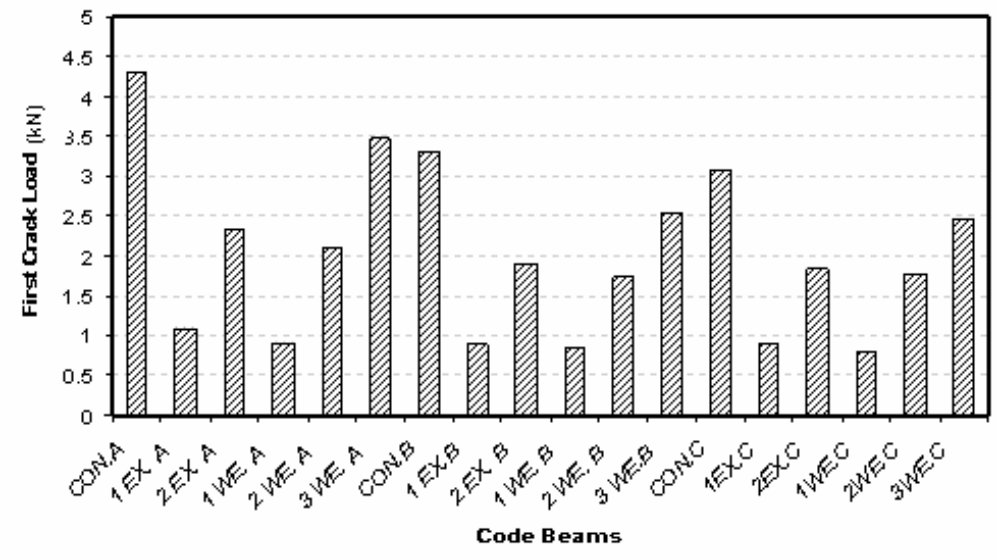

Figure 10: initial crack Load for all test specimens

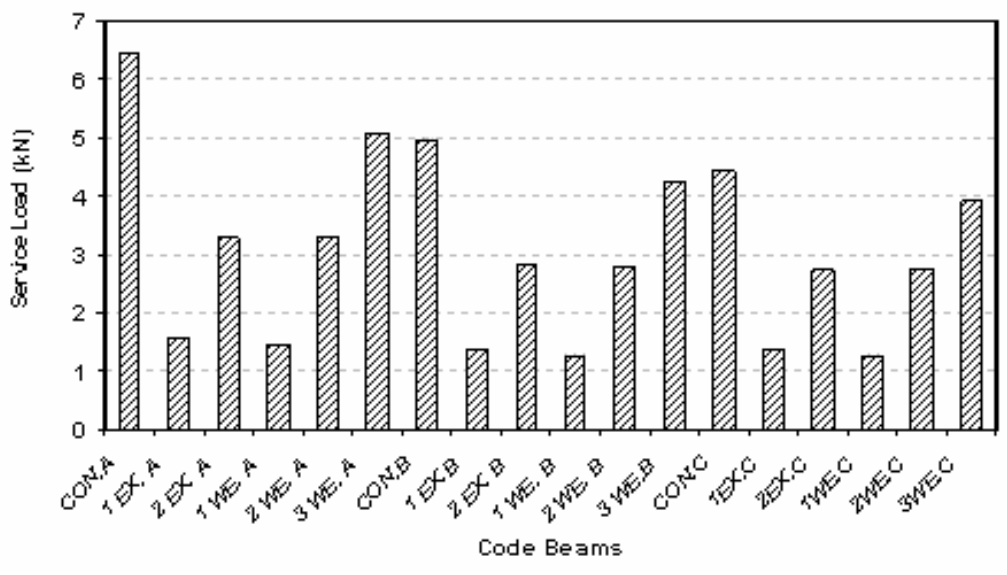

Figure 11.Service Load for all test specimens

10.2 Ultimate Load

Although a saving in the total reinforcing steel weight was achieved when the permanent ferrocement with single layer of steel mesh was used, Table 6 shows that ultimate load enhancement was achieved regardless of the type of the steel mesh in the ferrocement laminate. For single layer steel mesh, the saving in the weight of the steel mesh was about 73.2%, and 60.97% for the expanded steel mesh, and square mesh respectively. The percentage of decrease in the ultimate load was about 75% and 76.3% for the two types of the steel mesh respectively for group A. In group B, the percentage of decrease in the ultimate load was about 71.14 % and 74 % for the two types of the steel mesh respectively. In group C, the percentage of decrease in the ultimate load was about 72 % and 75% for the two types of the steel mesh respectively.

For the beams incorporating permanent ferrocement forms reinforced with double layers of steel mesh, there the saving in the weight of the steel mesh was about 53.7 % for the expanded steel mesh, and square mesh respectively. The percentage of decrease in the ultimate load was about 46.3 % and 48.3 % for the two types of the steel mesh respectively for group A. In group B, the percentage of decrease in the ultimate load was about 44.1 % and 46.82 % for the two types of the steel mesh respectively. In group C, the percentage of decrease in the ultimate load was about 42.93 % and 44.1 % for the two types of the steel mesh respectively.

For the beams incorporating permanent ferrocement forms reinforced with three layers of steel mesh, there the saving in the weight of the steel mesh was about 41.46% for the square mesh. The percentage of decrease in the ultimate load was about 16.47 % square meshes for group A. In group B, the percentage of decrease in the ultimate load was about 20.5 % for square mesh. In group C, the percentage of decrease in the ultimate load was about 15.7 % for square mesh. The decrease in the ultimate load for the beams incorporating ferrocement forms could be attributed to existence of area steel mesh, on the tension side of the beams as compared to the control specimens which had steel bars only. Figure 12 shows the ultimate cracking load for all tested beams.

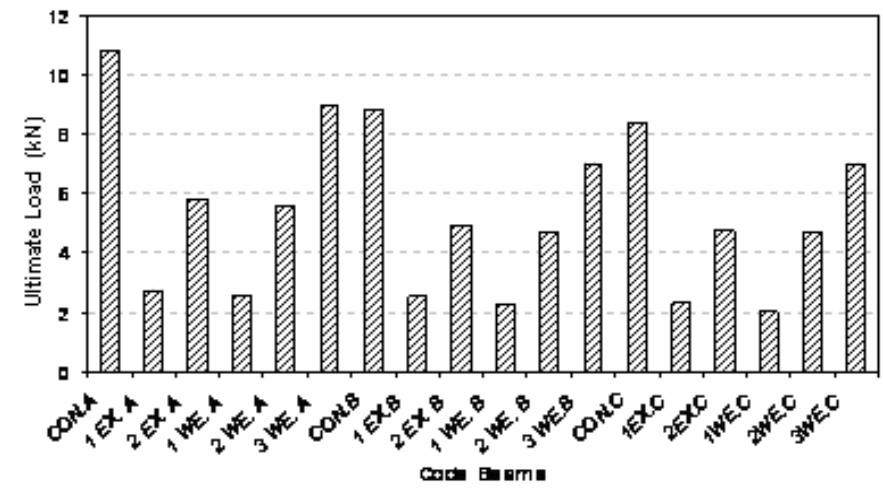

Figure 12: Ultimate Load for all test specimens

10.5 Ductility Ratio and Energy Absorption

Table 6 shows the calculated ductility ratio and energy absorption for all tested groups. As shown in Table 6, and figures 13 and 14. All of the tested beams had high ductility ratio. The ductility ratio for the test groups ranged from 4.27 to 13.07. Reduction of the ductility ratio occurred when permanent ferrocement steel forms were used. Although most of beams incorporating ferrocement forms attained large deflection at failure, the increase of the first crack load and its corresponding deflection resulted in this reduction of the ductility ratio, as defined in this investigation, in comparison to the control beam.

The energy absorption of beams incorporating the ferrocement permanent forms was lower than that of the control. The percentage of decrease of the energy absorption

relative to the control beams was about 89.95 % and 86.95% for group (A), 86.93 % and 87.43 % for group (B) and 88.93% and 92.3 % for group (C) when single layer of steel mesh was used. The percentage of decrease of the energy absorption relative to the control beams was about 63.0 % and 78.9 % for group (A), 69.7 % and 74.2 % for group (B) and 72.5.9% and 80.8 % for group (C) when double layer of steel mesh was used for Expanded chicken (hexagonal) and square steel mesh respectively. The percentage of decrease of the energy absorption relative to the control beams was about 62.7 % for group (A), 65.3 % for group (B) and 67.9 % for group (C) when tripe layer of square steel mesh was used.

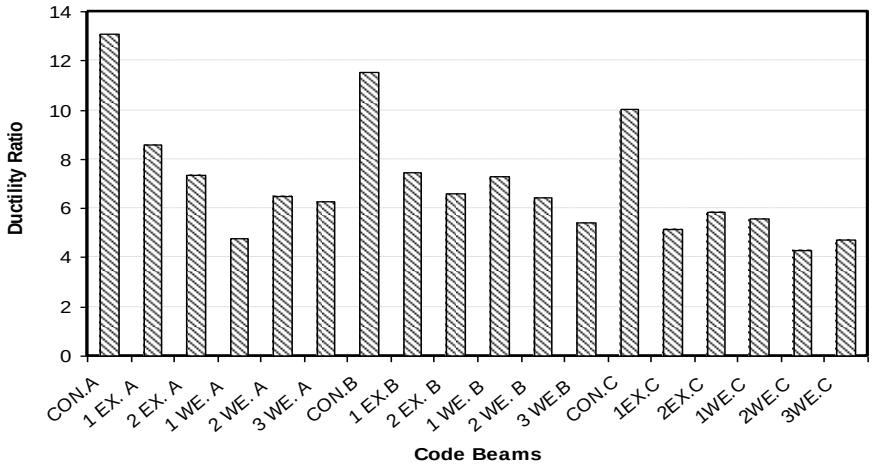

Figure 13: Ductility Ratio for all test specimens

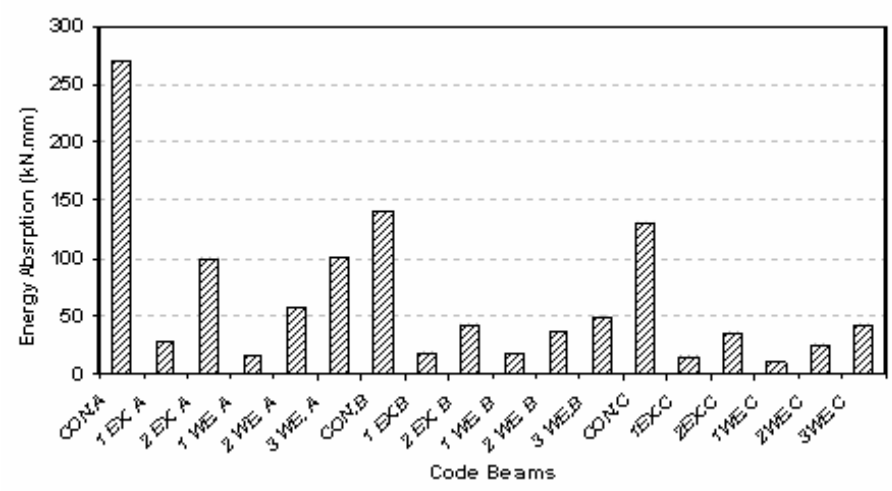

Figure 14. Energy Absorption for all test specimens

10.4 Cracking Behavior

Figure 15 shows the cracking patterns of the different test groups. For the control specimens, cracking started at mid-span. As the applied load increased, the developed cracks propagated rapidly from the tension side towards the compression side and spread along the beam span. At failure, cracks were wider than those for the beams incorporating permanent ferrocement forms. For the beams reinforced with Steel mesh, the first crack

occurred nearly at mid-span. The first crack load varied with the variation of the steel mesh type as shown in Table 6. As the load increased, new cracks developed at both sides of the first crack, while the first crack propagated vertically. New cracks developed with the additional increase of the load, while the previously developed cracks propagated nearly vertically. This pattern of crack development continued till failure of the beams. The number of the developed cracks varied with the variation of the steel mesh type. The failure mode for the tested beams changed flexure failure. All beams cracked in the early stages of loading in the maximum moment region within the middle third of the beam. In the reinforced concrete beam the flexure cracks propagated upwards with loading and followed by shear cracks near the supports in the shear zone. The crack width for the beams incorporating ferrocement forms as compared to the control beams could be attributed to the existence of the closely spaced steel mesh in the ferrocement forms.

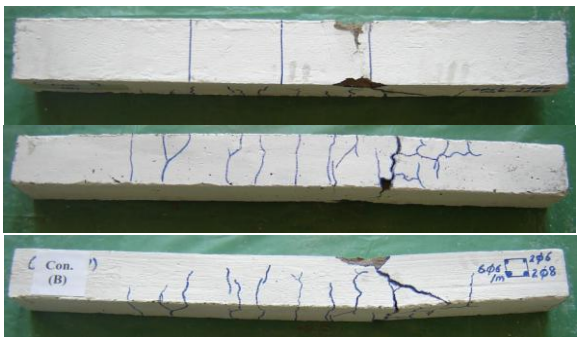

(a) Reinforcing concrete beam (con.)

(b) Single layer of Expanded mesh (EX)

(c)Double layer of Expanded mesh (EX)

(d) Double layer of square mesh (WE)

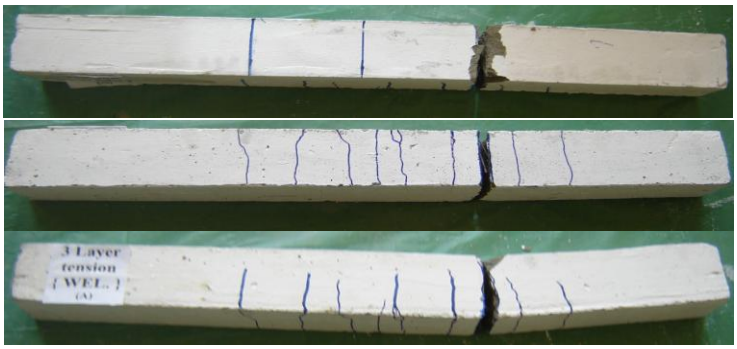

(e) Three layer of square mesh (WE)

Figure 15: Cracking Pattern of Test Beams

11. Verification of design equations

The nominal moment capacity M_n associated with significant concrete was predicted for the test beams applying ACI code [12,19] design equations and the calculated moment capacity were reported in Table (6). It can be seen that equations representing a simple formula adopted by the ACI code was the most conservative in predicting the nominal moment capacity. The more detailed ACI equations provided more accurate predictions.

12. Conclusions

Based on the results and observations of the experimental investigation presented in this paper, the following conclusions could be drawn:

1. Steel wire meshes offer numerous advantages over steel reinforcement, especially for structures with complex shapes and curvatures, because they are lighter, easier to handle, easier to cut, and easier to bend than steel reinforcement,.
2. The concrete beams incorporating permanent ferrocement forms, irrespective of the type of the steel mesh and number of layers in the ferrocement laminate, have a good strength, crack resistance, and energy absorption properties relative to conventional reinforced concrete beams of the same dimensions and total reinforcing steel content.
3. Although reduction in the ductility ratio, as defined in this research, occurred when permanent ferrocement was used relative to the control beams, all beams incorporating ferrocement forms still exhibited large deformation before failure and had large ductility ratios.
4. The concrete beams incorporating ferrocement forms reinforced with expanded hexagonal steel mesh exhibited the highest first crack load and serviceability load followed by the beams reinforced with square welded steel mesh.
5. Ultimate load for beams reinforced with expanded hexagonal steel mesh exhibited much higher responses than those reinforced with welded square steel mesh. This increase is due to the difference in the ultimate stresses of the two types of steel meshes and the volume fraction corresponding to each type.
6. Cracks with greater number and narrower widths were observed for those beams reinforced with steel meshes compared with beams reinforced with steel reinforcement.
7. Regarding its light weight, low cost, high ductility, steel meshes of particular relevance to ferrocement include satisfied strength, lower unit weight, ease of coiling and handling, and good properties.
8. The overall results demonstrate good performance for the beams reinforced with steel meshes due to fire.
9. The experimental nominal moment capacity was safely estimated by the ACI 318-11 code design equations.

13. References

[1] Rajkumar D. and Vidivelli B., *Performances of SBR Latex Modified Ferrocement for Repairing Reinforced Concrete Beams*, Australian Journal of Basic and Applied Sciences, Vol.4, (3), 2010, PP 520-531

[2] Al-Rifaei, Wail N. and Hassan, Arsalan H. *Structural Behavior of Thin Ferrocement One-way Bending Elements*. Journal of Ferrocement, Vol. 24, (2), 1994, PP115-126.

[3] Ohama, Y. and Demura K., *Pore size distribution and Oxygen diffusion resistance of Polymermodified mortars*, Cement and Concrete Research, Vol.21, 1991, PP 309-315.
[4] Fahmy, E.H., Shaheen, Y.B.I, and Korany, Y.S. *Repairing Reinforced Concrete Columns Using Ferrocement Laminates*, *Journal of ferrocement*, Vol.29 (2), 1999, PP 115-124.
[5] Fahmy, Ezzat H., Shaheen ,Yousry B., Abou Zeid, Mohamed N., and Gaafar, Haasan.. *Development of Ferrocement Panels for Floor and Wall Construction*. Proceedings of the 5th Structural Specialty Conference of the Canadian Society for Civil Engineering, Saskatoon, Saskatchewan, Canada. ST218-1 – ST218-10, 2004.
[6] Fahmy, Ezzat H., Abou Zeid, Mohamed N, Shaheen ,Yousry B., and Gaafar, Haasan.. *Behavior of Ferrocement Panels Under Axial and Flexural Loadings*. Proceedings of the 33rd Annual General Conference of the Canadian Society for Civil Engineering, Toronto, Ontario, Canada. GC150-1 – GC150-10, 2005.
[7] Jumaat, M.Z. and Alam, A., *Flexural Strengthening of Reinforced Concrete Beams Using Ferrocement Laminate with Skeletal Bars*, Journal of Applied Sciences Research, Vol.2(9), 2006, PP.559-566
[8] kazemi M. T. and morshed R., *Seismic shear strengthening of RC columns with ferrocement jacket*, Journal of structural Engineering, Vol. 1, 2005.
[9] Abang, A., *Application of ferrocement as a low cost construction Material in Malaysia. Journal of Ferrocement*. Vol. 25(2), 1995, PP 123-128.
[10] Djaknoun S., Benyahia A. and Ouedraogo E., *Characterization of the tenacity of the concrete mortars exposed to elevated temperatures*. American Journal of Applied Sciences Vol.6, (2), 2009, PP 296-308.
[11] Greepala V., Parichatprecha R., Tanchaisawat T. and Nimityongskul P., *Specific heat capacity of ferrocement using inverse thermal analysis*. RSID6- STR-10, 2009.
http://fscieng.csc.ku.ac.th/~ce/images/stories/paper/vatwong_rsid_str10.pdf. (Accessed at 8-2011)
[12] ACI 549.2R, *Report on thin reinforced cementitious products*, American Concrete Institute Farmington Hills, Michigan. ACI 5492R-04, 2004.
[13] Naaman A E., *Ferrocement and laminated cementitious composites*. Ann Arbor, Michigan, USA: Techno Press. Materials and Structures, Vol. 33, No. 2, 2000
[14] Greepala V. and Nimityongskul P., *Influence of heating envelope on post-fire mechanical properties of ferrocement jackets.* Asian Institute of Technology, Pathumthani 12120, Thailand. Vol. 12(3) , 2007
[15] Greepala V. and Nimityongskul P., *Structural integrity and insulation property of ferrocement exposed to fire*. Eighth International Symposium and Workshop on Ferrocement and Thin Reinforced Cement Composites Bangkok, Thailand, February 6-8, 2006.
[16] *Standard Test Methods for Fire Tests of Building Construction and Materials*" Annual Book of ASTM Standards, Vol 04.07. Designation ASTM E119-12.
[17] Fire-resistance tests-Elements of building construction; Part 3: Commentary on test method and guide to the application of the outputs from the fire-resistance test ISO/TR 834-3:2012
[18] *Fire tests on building materials and structures. Guide to the principles, selection, role and application of fire testing and their outputs* BS 476-10:, 2009, December 2008
[19] ACI Building Code *Requirements for Structural Concrete* (ACI318-11) and Commentary (ACI 318R-11), American Concrete Institute, P.O. Box 9094, Farmington Hills, Michigan, August 2011.
[20] RAMADAN A. G. *behavior of ferrocement concrete beams subjected to* fire. M.Sc. Thesis in Engineering - Civil Engineering Department – Menofiya University**,** Egypt, 2009.